Left and right tunnelling times of electrons from quantum wells in double-barrier heterostructures investigated by the stabilization method

1994 J. Phys.: Condens. Matter 6 887

(http://iopscience.iop.org/0953-8984/6/4/008)

J. Phys.: Condens. Matter 6 (1994) 887–898. Printed in the UK

Left and right tunnelling times of electrons from quantum wells in double-barrier heterostructures investigated by the stabilization method

J A Porto†, J Sánchez-Dehesa†, L A Cury‡, A Nogaret‡ and J C Portal‡

† Departamento de Física de la Materia Condensada, Facultad de Ciencias, Universidad Autónoma de Madrid, E-28049 Madrid, Spain

‡ INSA-CNRS, Departement de Physique, 31077 Toulouse and CNRS-SNCI, 38042 Grenoble, France

Received 12 July 1993, in final form 17 September 1993

Abstract. We present a numerical calculation of the tunnelling time of electrons confined in double-barrier structures performed by means of the so-called stabilization method, widely used in quantum chemistry. From the stabilization graphs we find the resonance energy and its width. The method is especially appropriate for treating the case of double-barrier structures (symmetric or non-symmetric) because it allows one to calculate separately the two different tunnelling times (to the left and to the right of the quantum well) contributing to the total lifetime of a resonant level. We use the effective-mass theory. The behaviour of the tunnelling time under applied bias is also investigated and the results are compared with the ones obtained by two alternative approaches, the quasi-classical approximation and the transmission coefficient analysis, respectively. A good agreement between the three methods is obtained for the cases analysed. Finally, the stabilization method as applied here can be employed in the field of scanning tunnelling microscopy of absorbed atoms or molecules where a double-barrier potential also serves as a model for the problem.

1. Introduction

The study of resonant tunnelling in semiconductor double-barrier structures (DBS) has been the subject of feverish activity since the pioneering work of Esaki and Tsu [1]. These structures have properties that are of technological interest, such as negative differential resistance and bistability in current–voltage response. Moreover, they are also of interest in basic research because they can be used as a tool to investigate the fundamental aspects of the tunnelling process. To obtain an up-to-date critical view of the work performed in this field one can consult the review by Hauge and Stovneng [2], and the recent review by Jauho [3]. We remark that resonant tunnelling phenomena also occur in scanning tunnelling microscopy, and the spectroscopy of absorbed atoms or molecules where a simple model of the problem gives a double-barrier-like potential configuration. In this last case the resonant levels are the corresponding atomic or molecular orbitals [4].

In recent years a number of papers have been devoted to the study of time scales for coherent tunnelling processes in different semiconductor structures. For example, the calculation of lifetimes of Stark resonant levels confined in a single quantum well (QW) has been performed using the effective mass theory [5–8]. Complicated effects that influence the escape rate in these rather simple structures, like Γ–X mixing or the details of band structure, have been worked out by other methods, namely the tight-binding method [9, 10]

0953-8984/94/040887+12$07.50

and the use of five $k \cdot p$ theory [11], respectively. Recently, the resonant energy and the width in symmetric double-barrier structures have been calculated in the simple effective-mass picture, even in the case of an applied electric field [12, 13]. In particular, in the case of a general DBS it is important to know what are the tunnelling probabilities associated with the two ways of escaping (to the left or to the right of the quantum well) that exist for the wavefunction of the quasi-confined level. On the other hand, many expressions obtained in the framework of elastic scattering theory require a knowledge of the partial elastic widths of these two channels of escape [14]. Up to now, when those magnitudes are needed a quasi-classical approximation is usually employed while the total lifetime is easily calculated by using a transmission coefficient analysis. In this paper we show that the stabilization method presents a unified scheme which allows one to calculate the total lifetime of electrons confined in the QW of DBS, as well as the magnitudes of their corresponding two partial tunnelling times. The energies of the resonant levels are calculated as well for a series of different symmetric and non-symmetric DBS. The paper is organized as follows. In section 2 we describe the stabilization method, in section 3 we write the formulae applicable in the quasi-classical approximation, in section 4 we analyse and compare the results obtained using the different approaches for some structures of current interest, and finally, in section 5, we summarize the present work.

2. The stabilization method

The stabilization method (SM) was developed in quantum chemistry as a general procedure for calculating resonance properties and wavefunctions for problems involving electron–atom and electron–molecule scattering [15]. The basic idea is to diagonalize the Hamiltonian in a basic set containing a scale factor η. The resulting eigenvalues as a function of η form what is called a stabilization graph (SG), which presents a characteristic pattern of avoided-crossings between stable and unstable eigenvalues, where the former correspond to the eigenvalues representing resonances and the latter to discretized continuum states. Macías and Riera [16] presented an explanation of why the SM works in the detection of resonances. Briefly, the simple explanation is the following. The wavefunction is well described for energies near the resonant energy and changes in the basis scarcely affect it. Therefore, the eigenvalues which are near the resonant energies are stable against variations in the basis set. In contrast, eigenvalues far from the resonant energy feel the modifications of the basis set because their wavefunctions are not well described in their greater part.

Of particular interest is the approximation developed by Simons [17], who was the first to propose that the values of the resonance position and its widths can be obtained directly from the SG. Simons used the assumption that the avoided-crossings that are typical in those graphs can be considered as equivalent to a linear crossing of the energies of two 'uncoupled' states, a stable and a 'continuum' one; in this way he was able to derive very simple expressions for both the resonance position and its width, depending just on the slopes of the stable and continuum eigenenergies. Thus, the resonance energy is just the diabatized crossing point between the stable and unstable eigenvalue.

With regard to the resonance width Γ, Borondo and Sánchez-Dehesa [7], and Macías and Riera [18] re-derived the Simons's formula by employing the standard golden-rule-type formulae yielded by the Feshbach [19, 20] formalism:

$$\Gamma = 2\pi\rho(E)V^2 \tag{1}$$

where the interaction term V is taken to be half the energy splitting at the pseudo-crossing ($\eta = \eta_i$) of the SG and $\rho(E)$ is the density of the 'continuum' states. If E_n is the discretized continuum eigenvalue interacting with the stable one, a good approximation for $\rho(E)$ [18] is

$$\rho(E) = \frac{2}{E_{n+1} - E_{n-1}}. \tag{2}$$

This formula is applicable if neither E_{n+1} nor E_{n-1} is contaminated by other stable eigenvalues. The accuracy of (1) and (2) for calculating Γ has been studied for different physical problems [7, 18].

At this point let us stress that the main point of the stabilization method is to generate the stabilization graph of the potential problem. This graph shows the behaviour, as a function of a non-linear parameter, of the eigenvalues of the Hamiltonian whose quasi-continuum has been discretized. This discretization is achieved in the standard formulation of the method by a scale factor η introduced in the basis set. Nevertheless, it can also be achieved by increasing the number N of localized wavefunctions employed in the Hamiltonian diagonalization, or by using any other suitable means which produce similar effects. For example, in the study of the quasi-bound spectra of quantum wells under an electric field [7] the discretization of the continuum outside the well is achieved by surrounding the system by infinite walls placed on both sides of the system (well and barriers), being the parameter the distance L between the walls. The SG was made up by varying that parameter; the energy levels for each L were calculated by diagonalizing the corresponding Hamiltonian. Afterwards, the resonance and its width were calculated from the graph following the above-mentioned guidelines.

2.1. The double-barrier structure under an applied bias

The calculation of the quasi-bound states localized in an idealized double-barrier structure is an exactly solvable problem. One can follow the standard method by matching the wavefunction and its first derivative at the interfaces. The final equation has a non-trivial solution only if the determinant of the coefficient matrix vanishes. All the roots obtained with this condition have negative imaginary parts; they have the form $E = E_0 - i\Gamma/2$, where E_0 and Γ correspond to the quasi-bound-state energy level and the resonance width, respectively. This procedure has been employed in [12], for the case of zero bias, and [13], in which the applied bias case is also studied but the linear dependence of the potential is extended to the collector and emitter sides. The main drawback of these calculations is that the total lifetime, τ_t, is obtained and, therefore, it is not possible to separate the contribution of the two different times, τ_l and τ_r, corresponding to the two possible ways of decay, through the left or right barrier, respectively. In what follows we apply the SM to this system and show how this method is especially appropriate to treat this problem because the two different times τ_l and τ_r can be calculated separately.

Following previous studies we reduce the initially three-dimensional problem to a one-dimensional effective-mass equation. We place the DBS between two infinite barriers placed at $z = 0$ and $z = L_1 + b_1 + w + b_2 + L_2$. The parameters involved, and the potential profile to solve, are shown in figure 1. We use an envelope-function approximation to describe the wavefunction of the particle confined in the structure

$$\phi(r) = u_{n,0}(r)\psi(z) \tag{3}$$

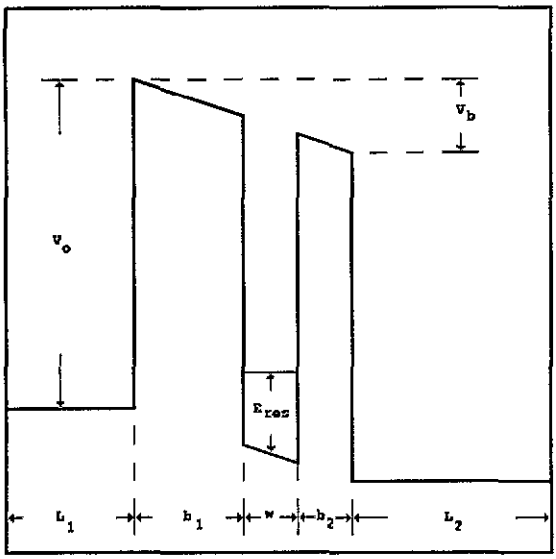

Figure 1. Potential diagram of a double-barrier structure under an applied bias. The parameters are described in the text.

where $u_{n,0}(r)$ is a Bloch state of zero wave vector and band index n; $\psi(z)$ is the envelope-function solution of the Schrödinger equation (in au):

$$
\begin{aligned}
&-\frac{1}{2m^*}\frac{d^2\psi}{dz^2} = E\psi \qquad 0 \leqslant z \leqslant L_1 \\
&-\frac{1}{2m^*}\frac{d^2\psi}{dz^2} + (V_0 - (z - L_1)F)\psi = E\psi \qquad L_1 \leqslant z \leqslant L_1 + b_1 \\
&-\frac{1}{2m^*}\frac{d^2\psi}{dz^2} - (z - L_1)F\psi = E\psi \qquad L_1 + b_1 \leqslant z \leqslant L_1 + b_1 + w \\
&-\frac{1}{2m^*}\frac{d^2\psi}{dz^2} + (V_0 - (z - L_1)F)\psi = E\psi \qquad L_1 + b_1 + w \leqslant z \leqslant L_1 + b_1 + w + b_2 \\
&-\frac{1}{2m^*}\frac{d^2\psi}{dz^2} - V_b\psi = E\psi \qquad L_1 + b_1 + w + b_2 \leqslant z \leqslant L_1 + b_1 + w + b_2 + L_2
\end{aligned}
\tag{4}
$$

where F is the electric field along the z direction, which is related to the applied bias, V_b, by

$$F = \frac{V_b}{b_1 + w + b_2}. \tag{5}$$

The barrier height V_0 is related to the alignment of the conduction band profiles at the Γ point of the Brillouin zone; $V_0 = \Delta E_c$. The system described by (4) has strictly bound states and has been solved by using a set of cubic-spline basis functions [21]. The advantage of this procedure is that it can be easily extrapolated to treat the cases of more realistic potentials in which the potential profile changes as a consequence of charge effects; then, the Poisson equation together with the Schrödinger equation have to be solved simultaneously.

In (4) the two parameters employed to get the corresponding SG are (i) the distance L_1 to the left-hand infinite barrier to obtain τ_l, and (ii) the distance L_2 to the right-hand infinite barrier to get τ_r. For example, in figure 2 we show the SG from which τ_r is calculated

for the case of a (Ga, In)As–(Al, In)As DBS under an applied bias $V_b = 100\,\text{meV}$ and parameters $b_1 = 70\,\text{Å}$, $w = 60\,\text{Å}$, $b_2 = 40\,\text{Å}$, $m^* = 0.041$, $V_0 = 500\,\text{meV}$. In this graph the energy levels for each L_2 are the eigenvalues obtained by diagonalizing the corresponding Hamiltonian given by (4). Looking at this graph it is possible to distinguish different kinds of levels according to their dependence on L_2. First we have those which present a completely flat behaviour (broken lines). They correspond to states fully localized on the emitter side, and have hold no interest at all. Second we have those which exhibit a certain dependence on L_2 (full curves). These levels are the interesting ones, and their dependence allows us to know the spatial region where they are mainly localized. The ones with the lineal dependence $\sim 1/L_2^2$ indicate that they are localized on the collector side; they belong to the continuum of the right side, which has been discretized. Finally, we have the levels localized inside the quantum well, the resonant levels, whose energies do not change with L_2 but present avoided crossings with the levels outside the well at certain values of the parameter. At these values the two energies are close, the levels interact and the two linear combinations of states, bonding–antibonding, are formed. This effect appears in the graph as an avoided-crossing region. This effect is shown in figure 3, where we plot a comparison between the wavefunctions of the same energy level obtained at two different values of the parameter L_2; one corresponding to a plateau ($L_2 = 100\,\text{Å}$) and the other at the crossing point $L_2 = 138.2\,\text{Å}$. Notice how the first one is the wavefunction associated with the quasi-confined level (full curve) while the one exhibiting huge oscillations out of the well (broken curve) indicates its combination with a discrete state of the right-hand part of the DBS.

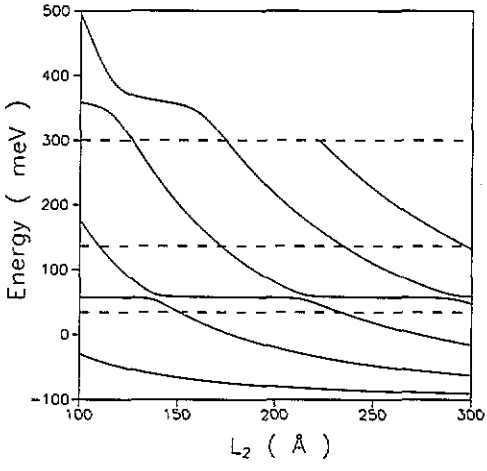

Figure 2. Stabilization graph of the two quasi-bound states allowed in a DBS based on (Ga,In)As/(Al,In)As (see text). The eigenvalues of (4) are represented against the separation L_2 between the right barrier and the infinite barrier put in the collector side. The broken lines correspond to energy levels confined on the left side of the structure.

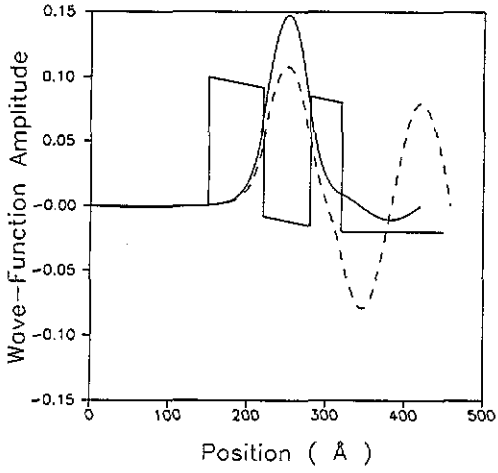

Figure 3. Comparison of the first resonant wavefunction at two different values of the parameter L_2 for the case considered in figure 2. The full curve corresponds to $L_2 = 100\,\text{Å}$ (non-crossing case) and the broken curve corresponds to $L_2 = 138.2\,\text{Å}$ (at the crossing point). The potential profile is also plotted.

Now, the energy of one quasiconfined level, E_{res}, as well as its lifetime can be obtained directly from the SG following the above-mentioned method. Briefly, this procedure consists

of selecting two energy curves, E_1 and E_2, which show an avoided crossing in the SG. They can be considered as solutions of a 2×2 secular problem whose diagonal elements are $E_{res}(L)$ and $E_c(L)$, the 'uncoupled' states, and $V(L)$ their interaction, where L is one of the above-described parameters (L_1 or L_2). This interaction is assumed to be localized near $L = L_c$ (the crossing point) and goes to zero in the regions where E_{res} = constant, and $E_c \sim 1/L^2$. The solution to this problem is

$$E_{1,2} = \tfrac{1}{2}\left(E_{res} + E_c \pm \sqrt{(E_{res} - E_c)^2 + 4V^2}\right). \tag{6}$$

To determine L_c we tabulate the function $R(L) = \frac{1}{2}(E_1 - E_2)$ and find its minimum. Therefore at L_c

$$E_{1,2} = \tfrac{1}{2}(E_1 + E_2) \pm V_c \equiv \epsilon \pm V_c \tag{7}$$

where $V_c = V(L_c) = \frac{1}{2}(E_1 - E_2)$. It is a good approximation to consider $E_{res} = \epsilon$ [7] as the energy of the resonance. An alternative is to take E_{res} as the energy value corresponding to regions of zero slope in the SG.

With regard to the lifetime, we calculate it in the complete coherent limit. We disregard any incoherent scattering process [14]. In the one-dimensional potential under study one can distinguish two independent and spatially separate channels of decay for the quasi-bound state in the quantum well of the DBS, to the left (l) and to the right (r), whose corresponding tunnelling times are $\tau_{l,r} = \hbar/\Gamma_{l,r}$ [22], where $\Gamma_{l,r}$ is given by (1) and (2). Finally, the total elastic width is $\Gamma_t = \Gamma_l + \Gamma_r$ and the decay rate of the resonant level is [14]

$$\frac{1}{\tau_t} = \frac{1}{\tau_l} + \frac{1}{\tau_r}. \tag{8}$$

We point out that, in the cases studied, we treat with a simple non-degenerate isolated long-lived Breit–Wigner resonance. For this reason, it is possible to use the above-mentioned equations for the energy width and the total lifetime in terms of the partial widths and partial tunnelling times, respectively.

In order to compare the accuracy of the results obtained with this method we have performed calculations for the same structures using a transmission coefficient analysis. In previous papers [23], Price has shown how the Lorentzian half-width at half-maximum of the transmission peak ΔE is related to the combined lifetime τ_t for tunnelling out of the well region through either of the enclosing barriers by

$$\frac{\hbar}{\tau_t} = 2\Delta E.$$

We have made this analysis by calculating ΔE with the formalism developed in [24]. The results obtained by both methods are similar, as we will show in section 4. We point out that the similitude of both methods comes from their coherent picture of the problem.

Another way of giving a comparison of our results is to adopt a different point of view. One can look at the problem as a classical particle (the electron) going back and forth inside the well, with a non-negligible probability of crossing the barriers given by the transmission coefficient of the corresponding barrier. This is the method used in the quasi-classical approach, which we describe below.

3. The quasi-classical approximation

The quasi-classical approach (QA) is widely used to calculate separately the magnitude of the tunnelling times on both sides of the QW sandwiched between barriers. The QA has been used to establish the order of magnitude of the charge accumulation inside the QW [25–27]. In practice, one has to take care of the condition for the quasi-classical approximation to be applicable (see for instance [28]). For the case of non-applied bias the transmission coefficient, $T_{l,r}$, through a barrier of length $b_{l,r}$ can be calculated using the Wentzel–Kramers–Brillouin (WKB) method (in au):

$$T_{l,r} = \mathcal{F} \exp\left[-2b_{l,r}\sqrt{2m^*(V_0 - E_{res})}\right] \tag{9}$$

where the prefactor $\mathcal{F}$ denotes the efficiency of the tunnelling process. The relation to the tunnelling time is [29]

$$\frac{1}{\tau_{l,r}} = \frac{v_{res}}{2w} T_{l,r} \tag{10}$$

where $v_{res} = (2E_{res}/m^*)^{1/2}$ and w is the nominal QW width. The coefficient of $T_{l,r}$ represents the number of times per second that the electron arrives to the corresponding barrier (left or right). Therefore, τ_l^{-1} (τ_r^{-1}) represents the rate of decay of the stored charge into unoccupied emitter (collector) states. For the case of applied bias

$$T_{l,r} = \mathcal{F} \exp\left(-\tfrac{4}{3}\sqrt{2m^*}\frac{\mp(V_0 - E_{res} \pm Fw/2)^{3/2} \pm (V_0 - E_{res} \pm Fb_{l,r} \pm Fw/2)^{3/2}}{F}\right) \tag{11}$$

where the upper (lower) sign corresponds to the case of transmission through the left-hand (right-hand) barrier considered as emitter (collector). F is the electric field defined by (5) and the resonant level is referred to the middle of the QW. In the formulae above one can use a simplified version of the WKB method with $\mathcal{F} = 1$ [30] and keep (11) as it stands. With these assumptions a good order of magnitude for the tunnelling time is found, as we will discuss in section 4. Nevertheless, one can get an improvement of those values if one takes into account the abruptness of the potential we work with, and the wave nature of the electrons. The first effect introduces a different factor in the transmission coefficient given by [28]

$$\mathcal{F} = 16(E_{res}/V_0)(1 - E_{res}/V_0). \tag{12}$$

On the other hand, by considering the wave nature of the electrons we slightly modify (11), introducing a larger length of the well given by

$$w_{eff} = w + d_l + d_r \tag{13}$$

in order to take into account the penetration length d_l (d_r) of the wavefunction in the left (right) barrier which are (in au):

$$d_{l,r} = \frac{3}{2}\frac{Fb_{l,r}}{\sqrt{2m^*}}\left[\mp(V_0 - E_{res} \pm Fw/2)^{3/2} \pm (V_0 - E_{res} \pm Fb_{l,r} \pm Fw/2)^{3/2}\right]^{-1} \tag{14}$$

where the upper (lower) sign is for the penetration length d_l (d_r) in the left-hand (right-hand) barrier close to the emitter (collector) side of the DBS.

4. Results and discussion

At this point let us remark on the simplifications we have used in the calculation with the above-explained models. First, we avoid any position dependence of the effective mass and effects of non-parabolicity in the conduction band dispersion. These effects have been analysed in these structures by other authors [24, 31, 32]. With regard to the effective-mass differences it has been proved that they produce observable effects in the measured currents only in the case where such differences are very high; for example, tunnelling from the Γ to X minima [32]. For the class of semiconductors which form the DBS to be studied, two of us [24] have proved that the resonant energy values obtained using a position mass dependence and non-parabolicity are practically the same as those obtained using just a homogeneous mass and without including the non-parabolicity (differences are of $\leqslant 2$ meV).

4.1. Symmetric and non-symmetric (Ga, In)As–(Al, In)As double-barrier structures

We use a $Ga_{0.47}In_{0.53}As$–$Al_{0.48}In_{0.52}As$-based DBS as the material to compare the tunnelling times obtained by the SM with those obtained by the other methods: the TC analysis and the QA, respectively. This system has a large conduction-band offset [33] ($V_0 = 500$ meV) and it is capable of confining two resonant levels in the QW. We take as the homogeneous mass $m^* = 0.041$, corresponding to the $Ga_{0.47}In_{0.53}As$ well [34] due to the above-explained reasons (see also [24]). Three different geometrical configurations of these semiconductors have been studied. The three have the same QW width ($w = 60$ Å) and differ in the length of the surrounding barriers: two have a symmetric configuration with $b_1 = b_2 = 40$ Å and 70 Å, respectively, and the non-symmetric one has $b_1 = 70$ Å and $b_2 = 40$ Å. In table 1 we show the values obtained for the total tunnelling escape time of the first resonant level $E_{res,1}$ for the symmetric 40–60–40 Å and 70–60–70 Å structures. To obtain the values shown in the column QA we first calculate the two separate times τ_r, τ_l by means of the formulae explained in section 3, using $\mathcal{F}$ given by (13) and the effective width w_{eff} (14). With regard to the SM values, the two times τ_r and τ_l are calculated separately and afterwards the formula (8) is applied to calculate the value of τ_t that appears in table 1. Finally, in the TC analysis ΔE is calculated as usual (see [24] for details) and afterwards the formula (9) is employed. Looking at table 1 one can conclude the equivalence of the three methods. We obtain very similar results with the SM and the TC analysis because of the reasons pointed out in section 2. Moreover, the results obtained with the QA are similar to those obtained with the SM or TC analysis because the energy difference $V_0 - E_{res,1}(V_b = 0) = 383.0$ meV is large, where the formulae of section 3 are in their range of applicability. Nevertheless, when the bias (V_b) grows, slight differences between the results obtained with the QA and the other two methods appear due to the decrease of the energy difference ($V_0 - E_{res}$). In figure 4(*a*) and (*b*) we plot the results obtained for τ_t as a function of the applied bias V_b. For the sake of comparison we have also included in these figures the values obtained by the QA using $\mathcal{F} = 1$ and the nominal width $w = 60$ Å in (11) and (12) (broken curve). As can be seen, using this approach the correct order of magnitude is reproduced, although the calculated values are a factor two higher than the results calculated with the SM and the TC analysis.

For the non-symmetric structure, the 70–60–40 Å DBS, we show in table 2 the comparison between the tunnelling times obtained for the first resonant level $E_{res,1}(V_b = 0) = 117.0$ meV, whose calculation is performed in similar conditions to those explained for the symmetric sample. Now, for clarity we separate the three tunnelling-times involved. In figure 5 we plot these same magnitudes as well as the comparison with the QA in the same condition as in figure 4(*a*) and (*b*). The conclusions are similar to those discussed

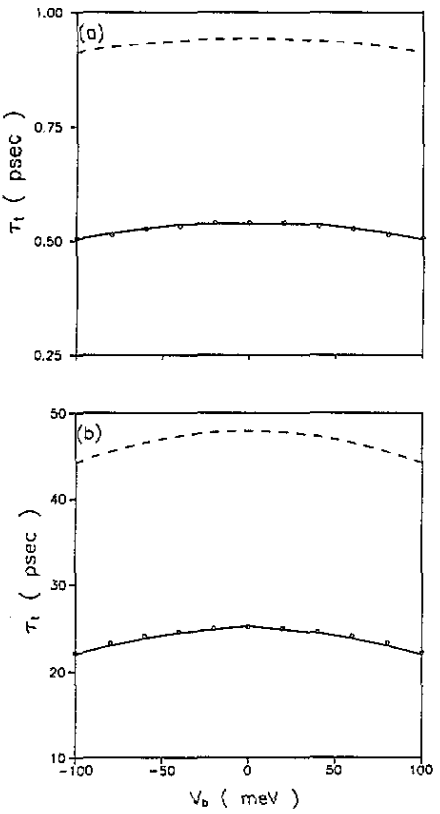

Figure 4. (*a*) Calculated total tunnelling time τ_t against applied bias V_b, for the first resonant state of a symmetric double-barrier structure (40–60–40 Å) based on (Ga,In)As/(Al,In)As. The full curve was obtained by the stabilization method and the circles by the transmission coefficient analysis. The broken curve corresponds to the quasi-classical approach using $\mathcal{F} = 1$ and the nominal well width in formula (11) (see text). (*b*) The same plots for the 70–60–70 Å structure.

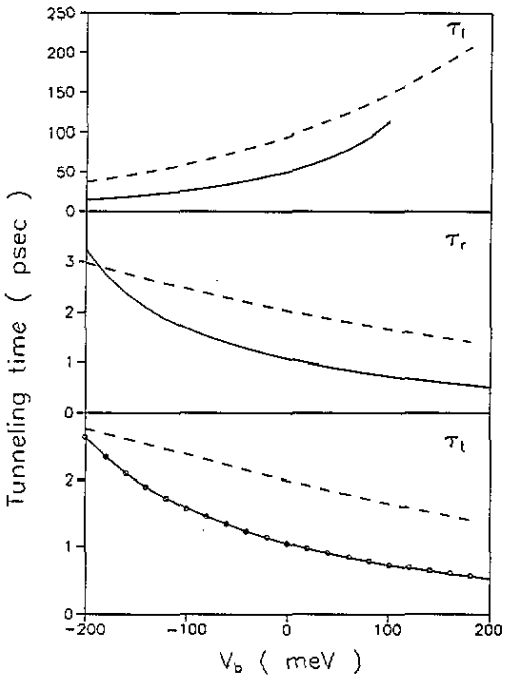

Figure 5. Calculated tunnelling times τ_l, τ_r and τ_t against applied bias V_b, for the first resonant state of a non-symmetric double-barrier structure (70–60–40 Å) based on (Ga,In)As/(Al,In)As. The full curve and circles were obtained by the stabilization method and the transmission coefficient analysis, respectively. The broken curve corresponds to the quasi-classical approach using $\mathcal{F} = 1$ and the nominal well width in formula (11) (see text).

Table 1. Comparison between the total tunnelling time τ_t (in ps) of the first resonant level calculated by means of the stabilization method (SM), the transmission coefficient (TC) analysis, and the quasi-classical approximation (QA) for two symmetric (Ga,In)As/(Al,In)As-based DBS at different applied bias.

	40–60–40 Å			70–60–70 Å		
V_b (meV)	SM	TC	QA	SM	TC	QA
0	0.538	0.539	0.539	25.2	25.3	25.4
40	0.536	0.533	0.536	24.6	24.7	25.1
100	0.504	0.506	0.522	22.0	22.2	23.5

previously for the symmetric DBS. We remark that the total tunnelling time is controlled by

the thin (right-hand) barrier, as could be expected. For the range of investigated bias, the tunnelling time for the thin barrier is at least an order of magnitude shorter than that for the thick (left-hand) barrier.

Table 2. Values (in ps) of the different tunnelling times at several applied voltages for the first resonant level in a non-symmetric 70–60–40 Å (Ga,In)As/(Al,In)As-based DBS calculated by means of the stabilization method (SM) and the quasi-classical approach (QA). The time τ_t obtained by the transmission coefficient (TC) analysis is also included (see text).

	SM			QA			TC
V_b (meV)	τ_l	τ_r	τ_t	τ_l	τ_r	τ_t	τ_t
−100	26.1	1.68	1.58	32.1	1.31	1.26	1.57
−40	39.0	1.27	1.23	42.4	1.17	1.14	1.23
0	50.4	1.07	1.05	50.8	1.08	1.06	1.05
40	68.0	0.91	0.90	60.6	0.99	0.98	0.91
100	114	0.73	0.73	78.6	0.88	0.87	0.73

Table 3. Comparison between the values (in ps) of the total tunnelling time of the first resonant level calculated by means of the stabilization method (SM) and the quasi-classical approach (QA) for an AlAs/GaAs/AlAs-based DBS for two different barrier heights V_0. The data in the column marked "Exp." are taken from figure 5 of [35] for $T = 20$ K.

	$V_0 = 960$ meV		$V_0 = 1360$ meV		
b_1(Å)–w(Å)–b_2(Å)	SM	QA	SM	QA	Exp.
28–62–28	9.46	9.39	47.9	48.0	~ 60
34–62–34	42.3	42.3	295	295	~ 160
40–62–40	191	191	1810	1810	~ 200

With respect to the second resonant level, $E_{res,2}(V_b = 0) = 418.7$ meV we have found a tunnelling escape rate two orders of magnitude lower than those obtained for the first resonance: for example, at $V_b = 100$ meV (the SG is represented in figure 2) the tunnelling times are 0.04, 0.04 and 0.06 ps obtained by the SM, TC and QA, respectively. Note that the differences between the results calculated with the QA and the other two methods (SM and TC) are larger for the second resonance than for the first one, due to a lower energy difference ($V_0 - E_{res,2}$).

4.2. Symmetric AlAs–GaAs–AlAs double-barrier structures

These kind of structures have been analysed by Tsuchiya and co-workers [35] by means of time-resolved photoluminescence spectroscopy. By analysing the behaviour of the decay time of the photoluminescence peak with temperature they are capable of determining the mechanism responsible for that decay: a tunnelling escape process or a radiative electron–hole recombination. They perform experiments with a series of symmetric samples with the same QW width ($w = 62$ Å) but different barrier lengths (28 Å $\leqslant b_1 = b_2 \leqslant 62$ Å). They found that for barriers thinner than 40 Å the decay times are almost independent of temperature, which indicates their non-radiative origin. These times can be compared with the calculated escape rates by tunnelling using the SM or the QA. In table 3 we give those numbers calculated using $m^* = 0.069$ and different barrier heights to consider different

proposals for the band-offset rule (1360 meV for the Dingle rule [36] and 960 meV for the Miller rule [37]). It is shown that both approaches give similar results for the analysed structures. The better agreement obtained by the Dingle rule does not necessarily imply that for GaAs/AlAs interfaces the conduction-band discontinuity is $\sim 0.85\Delta E_g$, where ΔE_g is the band-gap difference at the Γ point. On the contrary, it is currently accepted that the experimental value of that parameter is closer to $\sim 0.65\Delta E_g$ [38]. On the other hand, the agreement between the calculated results and the experimental measurements corresponding to the samples with non-radiative behaviour ($b_{1,2} < 40$ Å) can be considered satisfactory if one keeps in mind the uncertainty in the sample parameters as well as the effects, which are not considered here, that the inelastic events might play in these structures.

5. Summary

We have introduced the stabilization method of quantum chemistry to calculate in a coherent manner the resonant levels and the lifetimes of an electron in a QW of a double-barrier resonant structure under an applied electric field. We have applied the method to (In, Ga)As/(In, Al)As-and GaAs/AlAs-based double-barrier structures and the results have been compared with those obtained by two other methods of analysis: (i) the transmission coefficient analysis, and (ii) a quasi-classical approach. We have shown that the three methods give practically the same results for the samples investigated. Compared with the transmission coefficient analysis, the stabilization method has the advantage of giving us separately the two different tunnelling escape rates contributing to the total lifetime. Compared with the quasi-classical approach, it does not have its fundamental limitations. On the other hand, the comparison of the results obtained with the experimental ones available for the GaAs/AlAs structure indicates that the calculation describes satisfactorily the order of magnitude of the tunnelling times, and the discrepancies can be due either to non-elastic processes not considered in the calculation or to uncertainties in the sample parameters.

Finally, the stabilization method can be easily extended to treat the case of absorbed atoms or molecules in the field of scanning tunnelling microscopy, where similar double-barrier potentials describe the problem. The method is also capable of some improvements to analyse more realistic structures, where the charging effects should be considered by properly solving the Poisson and Schrödinger equations simultaneously.

Acknowledgments

We would like to thank F Flores for useful discussions. This work has been partially financed by the Comisión Interministerial de Ciencia y Tecnología of Spain under Contract Mat 91-0419 and by the Acción Integrada hispano-francesa HF-169.

References

[1] Esaki L and Tsu R 1970 *IBM J. Res. Dev.* **14** 61
[2] Hauge E H and Stonvneng J A 1989 *Rev. Mod. Phys.* **61** 917
[3] Jauho A P 1992 *Hot Carriers in Semiconductor Nanostructures* ed J Shah (New York: Academic) p 121
[4] Mizutani W, Shigeno M, Kajimura K and Ono M 1992 *Ultramicroscopy* **42–4** 236
[5] Austin E J and Jaros M 1985 *Phys. Rev.* B **31** 5569

[6] Austin E J and Jaros M 1985 *Appl. Phys. Lett.* **47** 274
[7] Borondo F and Sánchez-Dehesa J 1986 *Phys. Rev.* B **33** 8758
[8] Ahn D and Chuang S L 1986 *Phys. Rev.* B **34** 9034
[9] Schultz P A and Goncalvez da Silva C E T 1987 *Phys. Rev.* B **35** 8126
[10] Brey L and Tejedor C 1987 *Solid State Commun.* **61** 573
[11] Lassnig R 1987 *Solid State Commun.* **61** 577
[12] Bahder T B, Morrison C A and Bruno J D 1987 *Appl. Phys. Lett.* **51** 1089
[13] Peng J P, Chen H and Zhou S-X 1991 *Phys. Rev.* B **43** 12042
[14] Büttiker M 1988 *IBM J. Res. Dev.* **32** 63
[15] Taylor H S 1970 *Adv. Chem. Phys.* **18** 91
Hazi A U and Taylor H S 1970 *Phys. Rev.* A **1** 1109
[16] Macías A and Riera A 1985 *J. Physique* **46** 535
[17] Simons J 1981 *J. Chem. Phys.* **75** 2465
[18] Macías A and Riera A 1989 *Chem. Phys. Lett.* **164** 359; 1992 *J. Chem. Phys.* **96** 2877
[19] Feshbach H 1958 *Ann. Phys., NY* **5** 357
[20] Macías A and Riera A 1984 *Phys. Lett.* **103A** 377; 1985 *Chem. Phys. Lett.* **117** 42; 1986 *Europhys. Lett.* **2** 351
[21] Shore B W 1973 *J. Chem. Phys.* **58** 3855; 1973 **59** 6450; 1975 **63** 3935
[22] Galindo A and Pascual P 1990 *Quantum Mechanics* (Berlin: Springer)
[23] Price P J 1988 *Phys. Rev.* B **38** 1994; 1986 *Superlatt. Microstruct.* **2** 593
[24] Cury L A and Portal J C 1991 *Phys. Rev.* B **44** 6224
[25] Goldman V J, Tsui D C and Cunningham J E 1987 *Phys. Rev. Lett.* **58** 1257
[26] Sheard F W and Toombs G A 1988 *Appl. Phys. Lett.* **52** 1228
[27] Young J F, Wood B M, Ares G C, Devine R L S, Liu H C, Landheer D, Buchanan M, Springthorpe A J and Mandeville P 1988 *Phys. Rev. Lett.* **60** 2085
[28] Landau L D and Liftshitz E M 1976 *Quantum Mechanics* 3rd edn (Oxford: Pergamon)
[29] Weil T and Vinter B 1987 *Appl. Phys. Lett.* **50** 1281
[30] Jaros M 1989 *Physics and Applications of Semiconductor Microstructures* (Oxford: Clarendon)
[31] Ekenberg U 1989 *Phys. Rev.* B **40** 7714
[32] Ohno H, Mendez E E and Wang W I 1990 *Appl. Phys. Lett.* **56** 1793
[33] People R, Wecht K W, Alavi K, and Cho A Y 1983 *Appl. Phys. Lett.* **43** 118
[34] Alavi K, Aggarwal R L, and Groves S H 1980 *Phys. Rev.* B **21** 1311
[35] Tsuchiya M, Matsusue T and Sakaki H 1987 *Phys. Rev. Lett.* **59** 2356
[36] Dingle R, Wiegmann W, and Henry C H 1974 *Phys. Rev. Lett.* **33** 827
[37] Miller D A B, Chemla D S, Damen T C, Gossard A C, Wiegmann W, Wood T H, and Burrus C A 1984 *Phys. Rev. Lett.* **53** 2173
[38] Yu E T, McCaldin J O and McGill T C 1992 *Solid State Physics* **46** ed. H Ehrenreich and D Turnbull (New York: Academic) p 1